Life Sciences 231 (2019) 116549

Contents lists available at ScienceDirect

Life Sciences

journal homepage: www.elsevier.com/locate/lifescie

Long noncoding RNA TUSC7 inhibits cell proliferation, migration and invasion by regulating SOCS4 (SOCS5) expression through targeting miR-616 in endometrial carcinoma

Xiaoling Wu, Dongge Cai, Fan Zhang, Mu Li, Qiuyuan Wan*

Department of Obstetrics and Gynecology, The Second Affiliated Hospital of Xi'an Jiaotong University, Xi'an, Shaanxi 710004, China

ARTICLE INFO

Keywords:
Endometrial carcinoma
lncRNA TUSC7
miR-616
SOCS4/5
Cell proliferation
Cell cycle
Cell metastasis

ABSTRACT

Background: Long non-coding RNA (lncRNA) is emerging as an important regulator in various physiological and pathological processes. Recently, it was found that lncRNA long non-coding RNA tumor suppressor candidate 7 (TUSC7) could play tumor suppressive roles in several cancers. However, the function and underlying regulatory mechanism of lncRNA TUSC7 in endometrial carcinoma (EC) remains largely unclear.

Methods: The expression levels of TUSC7 and microRNAs-616 (miR-616) were analyzed by real-time PCR and *in situ* hybridization. Cell cycle and cell metastasis associated protein expressions were determined by western blotting. Cell proliferation, cycle and metastasis were determined by CCK-8 cell viability, colony formation, flow cytometer, wound scratch and transwell assays respectively *in vitro*. RNA pull-down, luciferase and western blotting assays were used to examine the target relationship between TUSC7 and miR-616 or that between miR-616 and suppressors of cytokine signaling 4 (5) (SOCS4 (SOCS5)). The functional effects of TUSC7 through sponging miR-616 were further examined using a xenograft tumor mouse model *in vivo*.

Results: TUSC7 was downexpressed in EC tissues and cell lines, and TUSC7 upregulation could remarkably inhibit cell proliferation, cycle progression and metastasis in EC cells. Mechanistic investigations demonstrated that TUSC7 can interact with miR-616 and decrease its expression, thereby upregulating the expression of miR-616's targets SOCS4 (SOCS5). Additionally, *in vivo* experiments using a xenograft tumor mouse model revealed that TUSC7 can serve as a tumor suppressor through sponging miR-616, and upregulating SOCS4 (SOCS5) in EC.

Conclusions: In this study, a newly identified regulatory mechanism of lncRNA TUSC7/miR-616/ SOCS4 (SOCS5) axis was systematically studied, which may hold promise as a promising target for EC treatment.

1. Introduction

EC, one of the three malignant tumors of the female reproductive tract, is an epithelial malignancy of the endometrium, whose onset is insidious and is prone to invasion and metastasis [1,2]. It is generally considered that EC incidence increases with age, along with worsen prognosis [3,4]. Recently, increasing number of long noncoding RNAs (lncRNAs) are being identified to regulate tumor-related gene expression at chromatin, genomic, transcription and post-transcriptional levels [5]. Therefore, exploring the role of vital lncRNAs in EC development may help to improve the early diagnosis rate, predict the prognosis and further improve the survival rate of EC patients.

TUSC7 composed of four exons and located on chromosome 3q13.3. Increasing evidences demonstrated that TUSC7 is down-regulated in most cancers and play a role of tumor suppressor [6–8]. For example, TUSC7 could inhibit the epithelial-mesenchymal transition progression in hepatocellular carcinoma through negatively regulating miR-10a [9]. TUSC7 overexpression inhibits glioma and gastric cancer development by targeting miR-23b [10–12]. Additionally, TUSC7 up-regulation suppresses the proliferation of lung cancer, colorectal cancer and osteosarcoma [13–15]. These studies showed that TUSC7 could play a tumor suppressive role through sponging some cancer-related miRNAs. In EC, Shang et al. showed that TUSC7 overexpression could increase the drug sensitivity [16]. However, its function and mechanism in EC development remains largely unclear.

MicroRNAs (miRNAs) are important regulators in multiple biological processes in cancer progression. As an important miRNA, miR-616 overexpression can induce androgen independent proliferation and enhance resistance to endocrine therapy by inhibiting TFPI-2 in prostate cancer cells [17]. miR-616 was also confirmed to be significantly

* Corresponding author at: Department of Obstetrics and Gynecology, The Second Affiliated Hospital of Xi'an Jiaotong University, 157 Xiwu Road, Xi'an, Shaanxi, China.

E-mail address: QiuyuanWan17@163.com (Q. Wan).

https://doi.org/10.1016/j.lfs.2019.116549
Received 7 January 2019; Received in revised form 4 June 2019; Accepted 7 June 2019
Available online 12 June 2019

upregulated in tumor tissues of gastric cancer patients [18]. Serum miR-616 level was reported to be significantly higher in lung adenocarcinoma patients than that in healthy persons [19]. In addition, miR-616 overexpression can inhibit cell apoptosis and promote tumor development in liver cancer [20], non-small-cell lung cancer [21], glioma [22]. Although the oncogenic function of miR-616 in most cancers has been reported, the role of miR-616 in EC has not been demonstrated.

As Src homology-2-containing proteins, SOCS consists of eight intracellular proteins (SOCS1–7 and the cytokine-induced Src homology-2 (SH2) protein) [23,24]. Each SOCS protein contains a central SH2 domain that interacts with phosphorylated tyrosines [25]. SOCS proteins compete with signal transducers and activators of transcription (STAT) protein for binding sites on activated cytokine receptors, and could bind janus kinase (JAK) protein to inhibit its tyrosine kinase activity [26]. Among them, SOCS-3 is frequently silenced by hypermethylation and could result in STAT3 inactivation and cell apoptosis [27]. SOCS-1 downregulation caused by promoter hypermethylation activates of JAK/STAT pathway in gastric cancer [28]. Other cancers whose development involved in the SOCS regulation included head and neck squamous cell carcinoma and colorectal cancer *et al* [29,30]. Specifically, SOCS4 acts as a novel gastric cancer suppressor gene using double combination array analysis [31], and SOCS5 mRNA and protein levels were down-regulated in thyroid gland cancer and liver cancer tissues [32]. However, little is known about SOCS4 and SOCS5 in EC. Previous study has revealed that IL-23 activated-miR-25 could suppress SOCS4 expression, further facilitate thyroid cancer cell migration and invasion [33]. However, the potential miRNAs holding promise as regulators of SOCS4 and SOCS5 in EC deserves further study.

In the present study, we determined the downexpression of TUSC7 in tissue samples of EC patients and studied TUSC7's effect on cell proliferation, cycle progression and metastasis. Through miRDB analysis, potential miRNAs that may be targeted by TUSC7 were predicted and confirmed by RNA pulldown assay. Additionally, as predicted by TargetScan, miR-616 may target the 3′-UTR of SOCS4 and SOCS5. Therefore, we speculated that TUSC7 might play a role in EC development by regulating SOCS4 and SOCS5 expression through modulating the level of miR-616. The function and regulatory mechanism of TUSC7/miR-616/SOCS4 (SOCS5) in EC progression were systematically studied *in vitro* and *in vivo*, which may provide a novel diagnostic and therapeutic candidate for EC treatment.

2. Materials and methods

2.1. Clinical samples

Fresh EC tissues and paired adjacent normal specimens were collected by surgical resection. The patients with EC had received neither chemotherapy nor radiotherapy prior to section. The procedures of this study were approved by the Institutional Review Board of The Second Affiliated Hospital of Xi'an Jiaotong University [34]. Signed informed consent was obtained from each patient. Pathological diagnostics for EC were independently determined by three pathologists. EC patient clinical information was listed in Table 1.

2.2. Cell culture

Human embryonic stem cell (ESC) and EC cell lines (HEC1A, HEC-1-B and Ishikawa) were purchased from ATCC cell lines (Manassas, USA). Gibco Essential 8 medium (Thermo Fisher Scientific, Rockford, IL, USA) without fetal bovine serum (FBS) was used for ESC culture. McCoy's 5a Medium (for HEC1A cells), Eagle's Minimum Essential Medium (for HEC-1-B cells) and Dulbecco's Modified Eagle Medium (for Ishikawa cells) supplemented with 10% FBS (Thermo Fisher Scientific) were used for EC cell culture. All cells were incubated in a humidified atmosphere of 5% CO_2 at 37 °C.

Table 1
Demographic data and clinical variables of EC patients.

Parameters total group	Number (total n = 120)	LncRNA TUSC7 expression low (%)	LncRNA TUSC7 expression high (%)	P value
Age (years)				
< 50	26	21(80.8)	12(19.2)	0.066
≥50	94	39(41.5)	48(58.5)	
Menstruation				
Non-menopause	32	18(56.3)	14(43.8)	0.409
Menopause	88	42(47.7)	46(52.3)	
FIGO stage				
I–II	66	26(39.4)	40(60.6)	0.01
III–IV	54	34(63.0)	20(37.0)	
Histological grade				
G1	62	24(38.7)	38(61.3)	0.011
G2 + G3	58	36(62.1)	22(37.9)	
Myometrial invasion				
< 1/2	53	21(39.6)	32(60.3)	0.043
≥1/2	67	39(53.7)	28(46.3)	
Lymphatic metastasis				
Yes	36	23(58.3)	13(41.7)	0.046
No	84	37(42.9)	47(57.1)	

2.3. RNA extraction and quantitative real-time PCR (qRT-PCR)

The TRIzol reagent (Thermo Fisher Scientific) was used to extract total RNA from the EC tissues and cultured cells. 1 μg total RNA was used as template for cDNA synthesis using a PrimeScript RT Reagent Kit (Takara, Shiga, Japan) according to the manufacturer's protocols. qRT-PCR assays for genes were performed using SYBR Premix Ex Taq (Takara). The expression of lncRNA TUSC7 was normalized to the expression of the β-actin level. A SYBR PrimeScript miRNA RT-PCR Kit (Takara) was used to examine miRNA levels. The expression of miRNAs was normalized to the expression of the U6 snRNA level. The information of primer sequences used in the analysis of qRT-PCR was listed in Table S1.

2.4. In situ hybridization (ISH) and immunohistochemical (IHC)

After the tissues were fixed in paraformaldehyde and paraffin-embedded, 5 μm sections were cut. For ISH, a peroxidase-labeled TUSC7 probe was obtained from (Thermo Fisher Scientific). ISH was performed with TUSC7 probe using an ISH kit for lncRNA detection (RiboBio, Guangzhou, China) according to manufacturer's instructions. The staining intensity was quantified using Image-ProPlus 6.0 by scanning 10 nonoverlapping fields in each section. Then, the mean intensity was calculated and served as an evaluation criterion for lncRNA TUSC7 expression “low and high”. Tissue was identified as “TUSC7 Low expression” if the section staining intensity was under the mean intensity. Accordingly, tissue was identified as“TUSC7 High expression” if the section staining intensity was higher than the mean intensity.

For IHC, The deparaffinized 5 μm sections were incubated with anti-Ki67, anti- SOCS4 (SOCS5) or anti-Vimentin antibodies (Cell Signaling Technology) at 4 °C overnight after antigen retrieval. The sections were then stained by the avidin-biotin-peroxidase complex using a Vectastain ABC kit (Vector Laboratories, Burlingame, CA). The peroxidase reaction was visualized by incubating the sections with 3-amino-9-ethylcarbazole solution, and counterstaining was carried out using Mayer's haematoxylin (Sigma-Aldrich, St. Louis, MO, USA).

2.5. Cell transfection

HEC1A or Ishikawa cells were transfected with TUSC7 expressing plasmid (lncRNA-TUSC7), TUSC7 siRNAs (siTUSC7-1, siTUSC7-2), miR-

616-5p-mimics (miR-616), miR-616-5p-inhibitors (miR-616-inh), SOCS4/5 expressing plasmid (SOCS4 (SOCS5)) or their corresponding controls (Con, siCon, miR-NC, NC-inh or Control) using a Lipofectamine 2000 transfection reagent (Thermo Fisher Scientific). The sequences of siRNAs for TUSC7 were listed in Table S2. The different kinds of cells were collected for qRT-PCR, wound scratch assay, cell invasion assay and luciferase reporter analysis 24 h after transfection, cell cycle assay or western blotting assay 48 h after transfection, or cell viability assay 0, 1, 2, 3, 4 days after transfection.

2.6. Plasmid constructs

The sequence of lncRNA TUSC7 was amplified using PCR with a human genomic DNA from HEC1A cells as the template. A One Step Cloning Kit ClonExpress II (Vazyme Biotech, Nanjing, P. R. China) was used. The sequence of lncRNA TUSC7 was then inserted into the *Kpn*I site of the PCI mammalian expression plasmids (Thermo Fisher Scientific) and verified using sequencing. According to the above methods, mammalian expression plasmids expressing SOCS4 or SOCS5 were respectively constructed. Additionally, the p-MIR-reporter plasmids (Promega, Madison, WI, USA) containing the 3′-UTR of SOCS4 or SOCS5 was constructed. The binding-site mutant luciferase plasmid (binding site: TTTTGAG replaced by AAAACTC for SOCS4, UUUGAG replaced by AAACUC for SOCS5) was also transfected as a control. The corresponding primer sequences for plasmid construct were listed in Table S3.

2.7. Cell proliferation assay

HEC1A or Ishikawa cells were respectively transfected with Con, lncRNA-TUSC7, siCon, si-TUSC7-1, si-TUSC7-2, miR-NC + Control, miR-616 + Control, miR-616 + SOCS4, miR-616 + SOCS5, Con + miR-NC, lncRNA-TUSC7 + miR-NC or lncRNA-TUSC7 + miR-616. The cells were then seeded onto 96-well plates at a density of 6×10^3 cells per well. After 0, 1, 2, 3, 4 days, the number of viable cells was detected using WST-8 staining with a Cell Counting Kit-8 (CCK-8, Dojindo, Tokyo, Japan). Absorbance was measured at 450 nm using a microplate spectrometer (Thermo Fisher Scientific).

2.8. Colony formation assay

HEC1A or Ishikawa cells (1×10^3) were mixed into 1.5 ml of top agar, and the top agar was then added onto base agar in each well. 2 ml complete medium was supplemented twice a week. After 3 weeks, colonies were stained with 0.5 ml of 0.1% Crystal Violet for 1 h, and colonies ≥ 0.5 mm were counted using a dissection microscope (TE2000-U, Nikon, Japan).

2.9. Cell cycle assay

HEC1A or Ishikawa cells were collected at 48 h post transfection. The cells were washed with PBS, fixed with 70% ethanol overnight, washed with PBS, resuspended in 400 μl of PBS and then incubated with 100 μg/ml RNase A (Takara) and 50 μg/ml propidium iodide (PI) (Sigma-Aldrich). Then, the cells were subjected to DNA content analysis using a FACSCalibur system (BD Biosciences, San Jose, CA) and the results were analyzed with the ModFit_LT software.

2.10. Protein extraction and western blotting

Protein from cells or tissues was extracted using RIPA lysis buffer (Sigma-Aldrich). The total protein content was quantified using a BCA protein assay kit (Thermo Fisher Scientific). Antibodies used in this study included p21, cyclinD1, E-cadherin, MMP2, MMP9, Vimentin, SOCS4, SOCS5, p-JAK1, p-STAT3, GAPDH and corresponding secondary antibodies. After incubated with the primary antibodies overnight at 4 °C, the membranes were incubated with a horseradish peroxidase-conjugated anti-mouse IgG (Thermo Fisher Scientific, 1:2000). The GAPDH level was used as an internal control for protein expression. More details of the antibodies used in this study are listed in Table S4.

2.11. Wound scratch assay

Linear scrape wounds were made on the cell monolayer when cells grown to confluence, and the wounds were allowed to heal for 24 h. Cell migration images were taken using an inverted microscope (Nikon). The distances from the edge to the middle of the scratch were determined using image J software (http://rsb.info.nih.gov/ij/).

2.12. Cell invasion assay

For cell invasion assay, 1×10^5 HEC1A or Ishikawa cells were plated into the top chamber of an insert (Corning Costar Co., Cambridge, MA, USA) precoated with 1 mg/ml matrigel (BD Bioscience, San Jose, CA, USA). Then, cells were cultured in the top chamber with serum-free medium, and medium supplemented with 10% FBS was used as an attractant in the lower chamber. After incubation for 12 h, the cells that migrated to the underside of the membrane were fixed with methanol, stained with crystal violet, imaged and counted.

2.13. RNA pull down assay

RNA pull down assay was performed as previously described [35]. Biotin-labeled lncRNA TUSC7 containing miR-616 binding site was transcribed from TUSC7 expressing plasmid with the Biotin RNA Labeling Mix (Roche, Indianapolis, IN, USA) and T7 RNA polymerase (Promega), treated with RNase-free Dnase I (Promega) and purified with a RNeasy Mini Kit (Qiagen, Valencia, CA). Biotinylated RNA was denatured at 95 °C, put in ice, left at room temperature to allow secondary structure formation, and then incubated with whole-cell lysates from HEC1A or Ishikawa cells at 25 °C. The lncRNA TUSC7-RNA complexes were isolated with Streptavidin agarose beads (Thermo Fisher Scientific) and the pull-down miRNAs was detected by qRT-PCR. Additionally, whole-cell lysates from HEC1A or Ishikawa cells were incubated with antibodies for Ago2, and the pull down complexes were subjected to RNA extraction and qRT-PCR analyses of lncRNA-TUSC7 and miR-616.

2.14. Luciferase reporter assay

When the cell confluence is at 70–80% in each well of 6-well plates, HEC1A or Ishikawa cells were co-transfected with the firefly luciferase reporter plasmid (1 μg), β-galactosidase expression vector (0.5 μg, Promega) and miR-616-mimic/Control (100 pmol) or lncRNA-TUSC7/Con (0.5 μg) using Lipofectamine 2000. The protein was extracted 24 h after transfection, and luciferase activities were tested using a Luciferase Reporter Assay System (Promega) according to the manufacturer's instructions.

2.15. Establishment of a mouse EC xenograft model

A mouse EC xenograft model was established in four-week-old thymic BALB/c male nude mice purchased from the Laboratory Animal Centre of Xi'an Jiaotong University Health Science Center (Xi'an, China). All animals received care according to the Guidelines for the Care and Use of Laboratory Animals published by the National Institutes of Health [36]. Firstly, HEC1A cells stably expressing lncRNA TUSC7 (lncRNA-TUSC7) or the corresponding control cells (Con) were constructed using a recombinant lentivirus expressing lncRNA TUSC7 or the control. Then, 1×10^6 stable cells in 100 μl PBS were injected subcutaneously into the right flanks of mice (5 mice/group). The

tumors were measured on 0, 1, 2, 3, 4, 5, 6, 7 and 8 weeks after injection. The tumor volume was calculated as $1/2LW^2$, where W and L are the smallest and the largest perpendicular tumor diameter, respectively. The mice were sacrificed, weighted and photographed at 8 weeks post-implantation. Additionally, the tumor tissues were collected for the analyses of Vimentin, Ki67, miR-616, SOCS4, SOCS5, p-JAK1 and p-STAT3 levels.

2.16. Statistical analysis

Experiments were conducted in triplicate and repeated at least three independent times. Results in this study are expressed as the mean ± standard error of the mean (SEM). Differences between two groups were analyzed using Student's *t*-test. The comparison between multiple groups was compared using one-way ANOVA. The correlations between TUSC7 and miR-616, miR-616 and SOCS4/5 protein levels, TUSC7 and SOCS4/5 protein levels were respectively analyzed by Pearson's correlation analysis. $p < 0.05$ was considered significant. $*/\#P < 0.05$; $**/\#\#P < 0.01$; $***/\#\#\#P < 0.001$.

3. Results

3.1. TUSC7 is decreased in EC tissues and cells

As shown in Fig. 1A, the qRT-PCR analysis revealed that the TUSC7 level was significantly decreased in 60 EC samples compared to normal adjacent tissue samples. The ISH data also indicated that TUSC7 downregulation is a common event in EC (Fig. 1B). As shown in Fig. 1C, TUSC7 levels in EC cell lines (HEC1A, HEC-1-B and Ishikawa) were lower than that in human embryonic stem cells (ESC). Particularly, relatively higher or lower level of TUSC7 was expressed in Ishikawa and HEC1A cells, respectively, which were used in the following studies. TUSC7 affects proliferation, cell cycle progression and metastasis of EC cells.

The results in Fig. 2A revealed that the TUSC7 level was markedly increased after transfected TUSC7 expressing plasmid (lncRNA-TUSC7) in Ishikawa and HEC1A cells compared to the control group. Inversedly, siRNAs (siTUSC7-1, siTUSC7-2) for TUSC7 in Ishikawa and HEC1A cells caused significantly decreased TUSC7 levels compared to the si-Congroup. The cell growth was inhibited in HEC1A and Ishikawa cells after TUSC7 was overexpressed and TUSC7 knockdown caused completely inversed results (Fig. 2B). The results of colony formation assay showed that TUSC7 overexpression significantly decreased colony numbers, and TUSC7 downexpression stimulated colony formation of Ishikawa and HEC1A cells (Fig. 2C). Additionally, as shown in Fig. 2D, TUSC7 overexpression in HEC1A and Ishikawa cells caused an increase in the G1-phase cell population and a decrease in the S-phase cell population. Adversely, in siTUSC7-transfected cells, a decrease in the G1-phase cell population and an increase in the S-phase cell population were showed. The western blot data in Fig. 2E showed that the expression levels of cell cycle associated proteins (p21, cyclinD1) were significantly altered after TUSC7 was dysregulated.

Furthermore, the effects of TUSC7 on EC cell metastasis were studied using wound scratch healing and transwell assays. The wound scratch healing results showed that the mobility of HEC1A and Ishikawa cells was significantly reduced after TUSC7 overexpression, and markedly enhanced after siTUSC7 transfection (Fig. 3A). As shown in Fig. 3B, the numbers of invaded HEC1A and Ishikawa cells with TUSC7 overexpression were significantly reduced, but the numbers of invaded cells with TUSC7 knockdown were significantly increased. In addition, the western blot data in Fig. 3C showed that the expression levels of cell metastasis-associated proteins (E-cadherin, MMP2, MMP9 and Vimentin) were significantly influenced after TUSC7 was dysregulated. These results indicated that TUSC7 could inhibit cell proliferation, colony formation, cell cycle progression and cell metastasis in HEC1A and Ishikawa cells.

3.2. TUSC7 directly binds to miR-616-5p and negatively regulate its expression

Based on these foundations the underlying molecular mechanism of TUSC7in EC was further explored. The potential miRNAs targeted by TUSC7 was predicted by bioinformatics analysis (miRDB, http://www.mirdb.org). The results showed that TUSC7 could potentially interact with miR-616-5p, miR-4419a, miR-4261, miR-4255 and miR-4773. The biotinylated TUSC7 harboring binding sites of these five miRNAs were synthesized *in vitro*. The RNA immunoprecipitation pulled down data in Fig. 4B showed that miR-616-5p could be significantly enriched by biotin-labeled lncRNA-TUSC7. However, miR-4419a, miR-4261, miR-4255 and miR-4773 could not be pulled down by lncRNA-TUSC7, suggesting the specific interaction between miR-616 and TUSC7 in Ishikawa and HEC1A cells. The results in Fig. 4C showed that both lncRNA-TUSC7 and miR-616 were significantly pulled down by antibody for Ago2 protein, which is a core component of miRNA-mediated RISC protein complex, further confirming the interaction between miR-616 and TUSC7. Accordingly, TUSC7 overexpression significantly decreased miR-616 level and TUSC7 knockdown markedly increased miR-616 level in Ishikawa and HEC1A cells (Fig. 4D). Additionally, the results in Fig. 4E showed that miR-616 level was significantly increased in EC tissue samples. The Pearson's correlation analysis indicated that miR-616 expression was negatively associated with TUSC7 levels in tissue samples of EC patients (Fig. 4F). These findings together revealed that TUSC7 can directly bind to miR-616 and regulate its expression in EC cells.

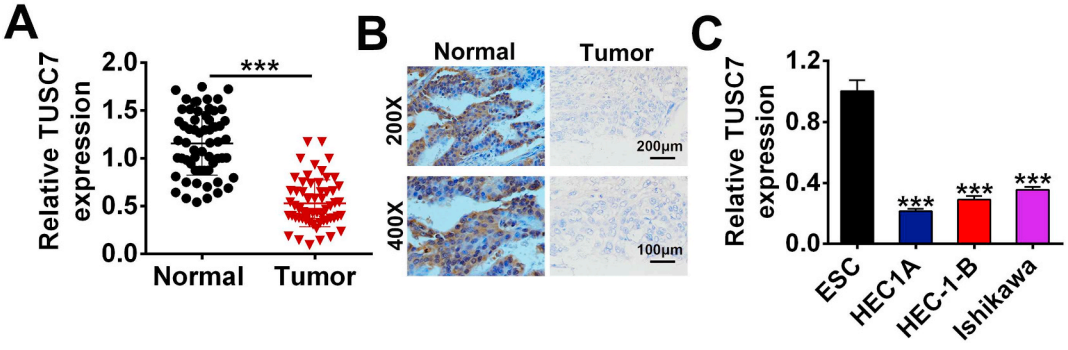

Fig. 1. TUSC7 is downregulated in EC tissues and cells. (A) The relative lncRNA TUSC7 expression levels in EC tissues (Tumor) and normal adjacent tissues (Normal), as determined using qRT-PCR. (B) The lncRNA TUSC7 expression levels in EC tissues (Tumor) and normal adjacent tissues (Normal), as determined using ISH (n = 120). (C) The relative lncRNA TUSC7 expression levels in human embryonic stem cell (ESC) and EC cell lines (HEC1A, HEC-1-B and Ishikawa), as determined using qRT-PCR. The data are expressed as the mean ± SEM, $***P < 0.001$.

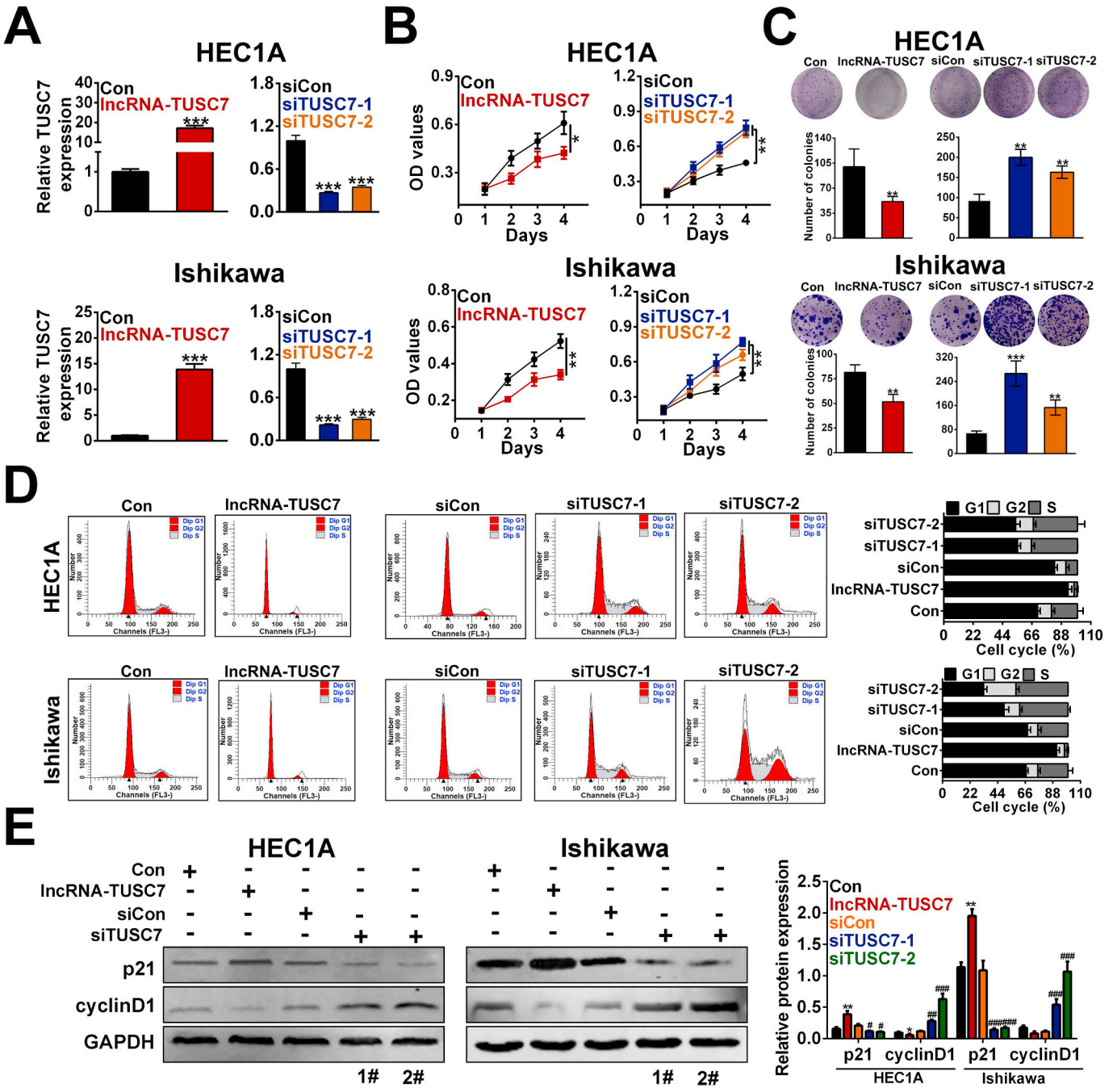

Fig. 2. TUSC7 effects the proliferation and cell cycle progression of EC cells. (A) The relative lncRNA TUSC7 expression levels in HEC1A or Ishikawa cells after transfection with lncRNA-TUSC7, siTUSC7-1, siTUSC7-2, or the corresponding control (Con, siCon), as determined using qRT-PCR. (B) Growth curves of HEC1A or Ishikawa cells after transfection with lncRNA-TUSC7, siTUSC7-1, siTUSC7-2, or the corresponding control (Con, siCon). The measurements of the cell growth rate were obtained using a CCK-8 kit. (C) Colony formation analysis of HEC1A or Ishikawa cells after transfection with lncRNA-TUSC7, siTUSC7-1, siTUSC7-2, or the corresponding control (Con, siCon). Colony numbers were quantified and shown as histograms. (D) Cell cycle analysis of HEC1A or Ishikawa cells after transfection with lncRNA-TUSC7, siTUSC7-1, siTUSC7-2, or the corresponding control (Con, siCon). Apoptosis rates were quantified and shown as histograms. (E) The protein levels of p21 and cyclinD1 in HEC1A or Ishikawa cells after transfection with lncRNA-TUSC7, siTUSC7-1, siTUSC7-2, or the corresponding control (Con, siCon), as determined using western blotting. Relatively quantitative results was determined by Image J and shown as histogram. The data are expressed as the mean ± SEM, */#$P < 0.05$; **/##$P < 0.01$; ***/###$P < 0.001$.

3.3. TUSC7 upregulates SOCS4 and SOCS5 protein levels and enhances the phosphorylation of JAK1 and STAT3 through inhibiting the miR-616 expression

Through bioinformatics analysis (TargetScan), we found that SOCS4 and SOCS5 were probably potential targets of miR-616 and the binding sites between miR-616 and SOCS4 (SOCS5) marked in red were depicted in Fig. 5A.. The miR-616 level was markedly increased after transfecting miR-616 mimics, and transfection of miR-616 inhibitor (miR-616-inh) caused significantly decreased miR-616 levels in Ishikawa and HEC1A cells (Fig. 5B). The western blot results in Fig. 5C demonstrated consistent results. Previous studies suggested that the endogenous regulatory family of SOCS controls the magnitude and duration of JAK/STAT signaling through several mechanisms, including

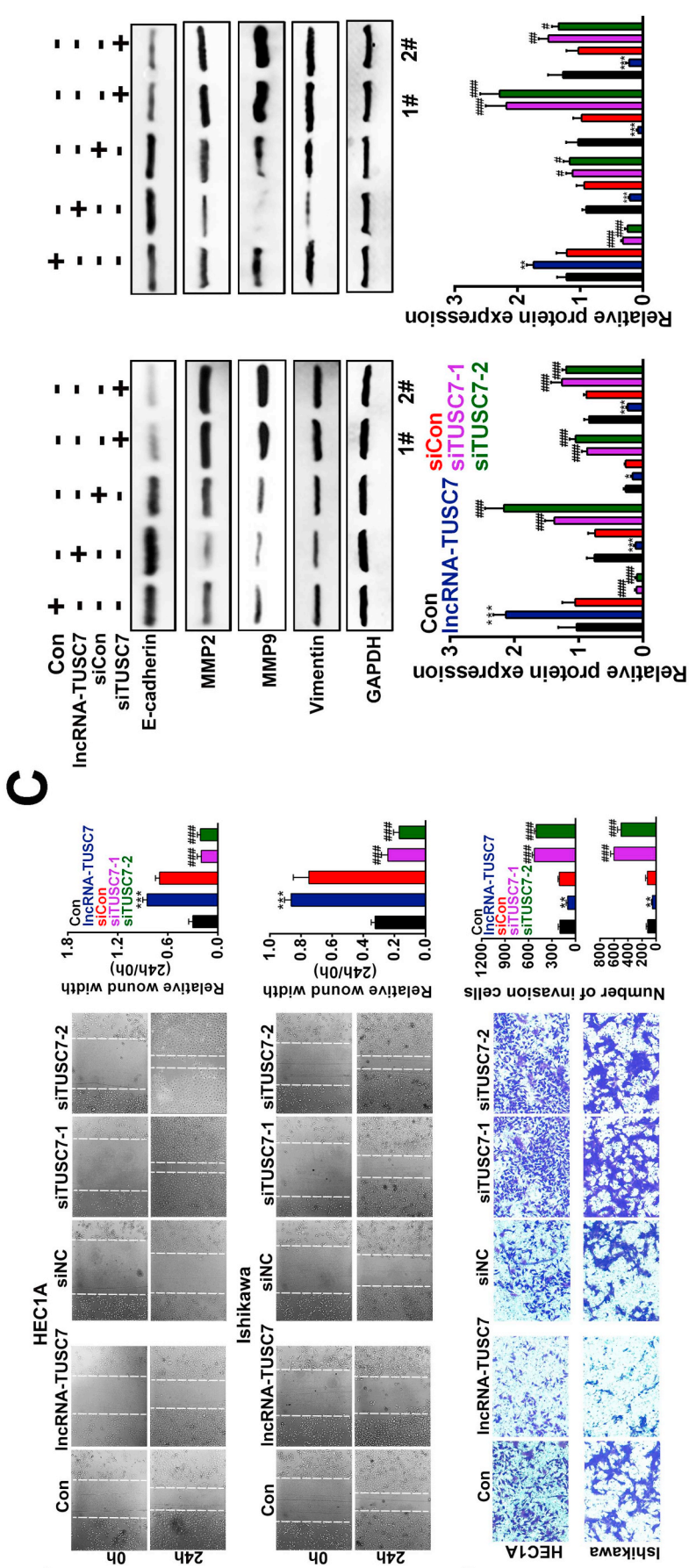

Fig. 3. TUSC7 affects the metastasis of EC cells. (A) Wound scratch healing assay of HEC1A or Ishikawa cells after transfection with lncRNA-TUSC7, siTUSC7-1, siTUSC7-2, or the corresponding control (Con, siCon). Quantification of the wound-healing assay was shown as histograms. (B) Representative invasion assay images of HEC1A or Ishikawa cells after transfection with lncRNA-TUSC7, siTUSC7–1, siTUSC7–2, or the corresponding control (Con, siCon). The invaded cells were quantified and shown as histograms. (C) The protein levels of E-cadherin, MMP2, MMP9 and Vimentin in HEC1A or Ishikawa cells after transfection with lncRNA-TUSC7, siTUSC7-1, siTUSC7-2, or the corresponding control (Con, siCon), as determined using western blotting. Relatively quantitative results was determined by Image J and shown as histogram. The data are expressed as the mean ± SEM, $*/\#P < 0.05$; $**/\#\#P < 0.01$; $***/\#\#\#P < 0.001$.

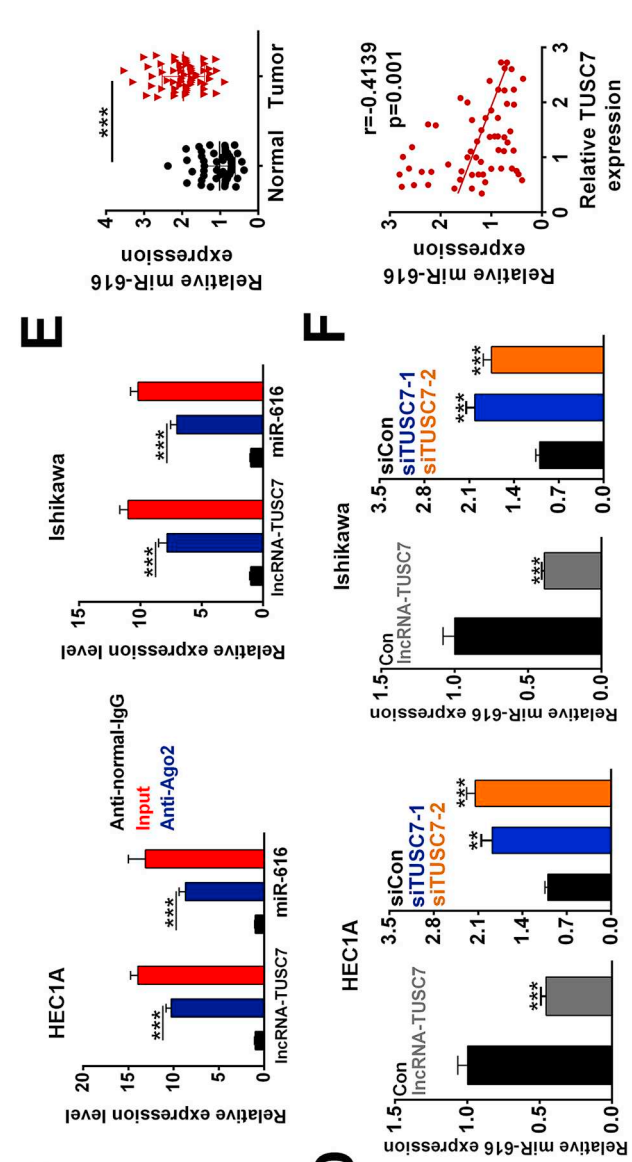

Fig. 4. TUSC7 directly binds to miR-616-5p and negatively regulate its expression. (A) miRDB prediction tools identified seeds match for TUSC7 in the mature sequence of miR-616-5p, miR-4419a, miR-4261, miR-4255 and miR-4773. The predicted seed-recognition site in the miRNA sequences and the corresponding TUSC7 sequence are marked in red. (B) HEC1A or Ishikawa cells were harvested and mixed with biotinylated TUSC7 to perform biotin-based pull down. miRNA enrichments were tested by qRT-PCR and compared to control. (C) HEC1A or Ishikawa cells were harvested and mixed with Ago2 antibodies to perform miRNA-based pull down. lncRNA or miR-616 enrichments were tested by qRT-PCR and compared to control. (D) The relative miR-616 expression levels in HEC1A or Ishikawa cells after transfection with lncRNA-TUSC7, siTUSC7-1, siTUSC7-2, or the corresponding control (Con, siCon), as determined using qRT-PCR. (E) The relative miR-616 expression levels in EC tissues (Tumor) and normal adjacent tissues (Normal), as determined using qRT-PCR. (F) Pearson's correlation scatter plot comparing the fold changes in the expression of miR-616 and lncRNA TUSC7 in EC patients. The data are expressed as the mean ± SEM, $^{***}P < 0.001$. (For interpretation of the references to color in this figure legend, the reader is referred to the web version of this article.)

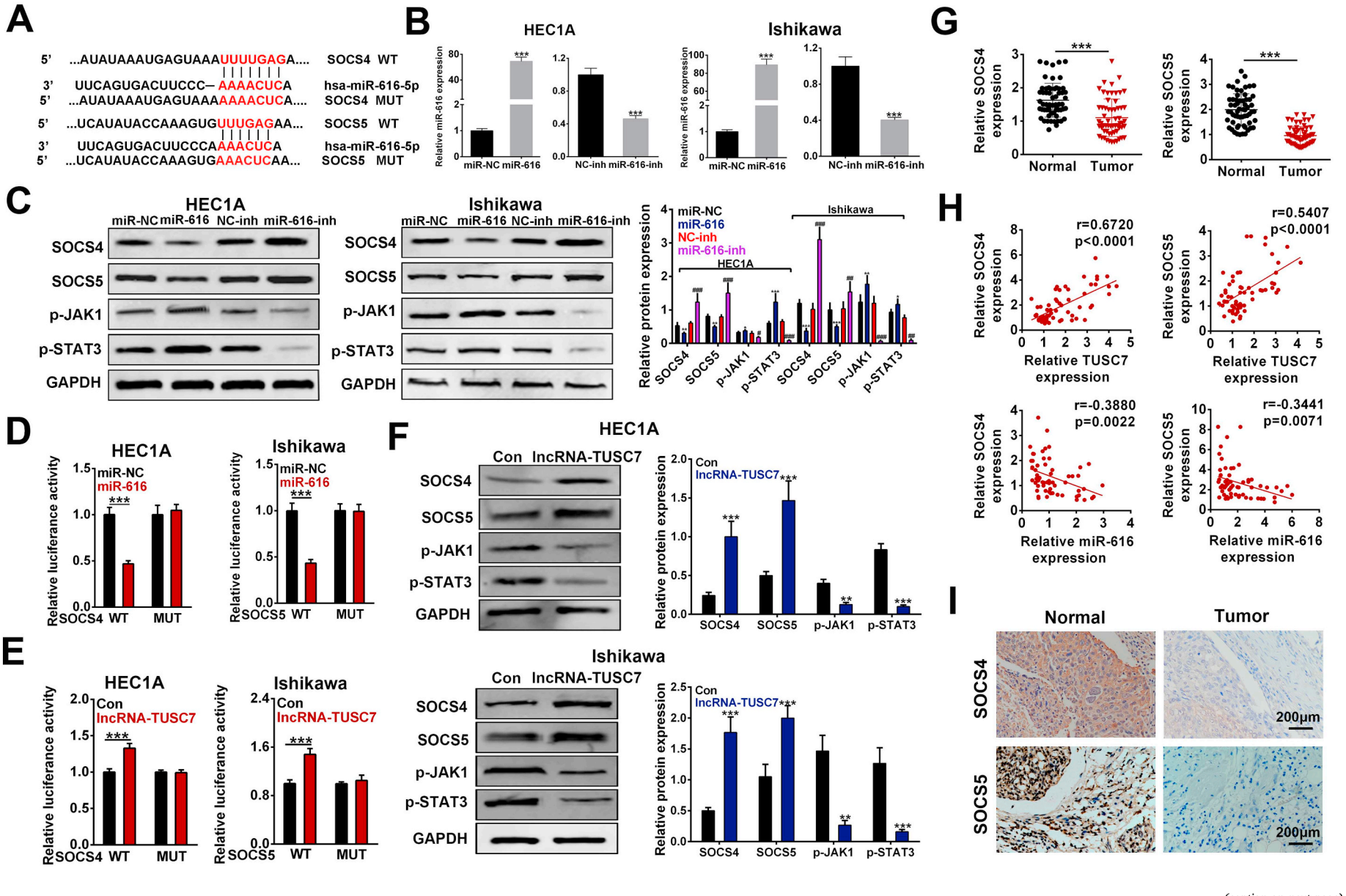

(caption on next page)

Fig. 5. TUSC7/miR-616 regulates SOCS4 and SOCS5 protein levels and the phosphorylation levels of JAK1 and STAT3. (A) TargetScan prediction software identified seeds match for miR-616-5p in the 3′UTR of SOCS4 and SOCS5; the predicted seed-recognition sites in the SOCS4 and SOCS5 mRNA sequence and the corresponding miR-616-5p sequence are marked in red. (B) The relative miR-616 expression levels in HEC1A or Ishikawa cells after transfection with miR-616 mimics (miR-616), miR-616 inhibitors (miR-616-inh) or the corresponding control (Con, siCon), as determined using qRT-PCR. (C) The protein levels of SOCS4, SOCS5, p-JAK1 and p-STAT3 in HEC1A or Ishikawa cells after transfection with miR-616 mimics (miR-616), miR-616 inhibitors (miR-616-inh) or the corresponding control (miR-NC, miR-616-inh), as determined using western blotting. Relatively quantitative results was determined by Image J and shown as histogram. (D) The relative luciferase activity of the SOCS4 or SOCS5 3′-UTR reporter plasmid was assayed in HEC1A or Ishikawa cells after transfection with miR-616 mimics (miR-616) or the corresponding control (miR-NC). The mutant SOCS4 or SOCS5 3′-UTR reporter was also used as a control. (E) The relative luciferase activity of the SOCS4 or SOCS5 3′-UTR reporter plasmid was assayed in HEC1A or Ishikawa cells after transfection with lncRNA-TUSC7 or the corresponding control (Con). The mutant SOCS4 or SOCS5 3′-UTR reporter was also used as a control. (F) The protein levels of SOCS4, SOCS5, p-JAK1 and p-STAT3 in HEC1A or Ishikawa cells after transfection with lncRNA-TUSC7 or the corresponding control (Con), as determined using western blotting. Relatively quantitative results was determined by Image J and shown as histogram. (G) The relative SOCS4 and SOCS5 protein expression levels in EC tissues (Tumor) and normal adjacent tissues (Normal), as determined using IHC. (H) Pearson's correlation scatter plot comparing the fold changes in the expressions of lncRNA TUSC7 and SOCS4 (SOCS5), miR-616 and SOCS4 (SOCS5) in EC patients. (I) The SOCS4 (SOCS5) protein expression levels in EC tissues (Tumor) and normal adjacent tissues (Normal), as determined using IHC. The data are expressed as the mean ± SEM, $^{**}P < 0.01$; $^{***}P < 0.001$. (For interpretation of the references to color in this figure legend, the reader is referred to the web version of this article.)

JAK inhibition, STAT binding and targeting for proteasomal degradation [37,38], we thus detected the expression of the phosphorylation of JAK1 and STAT3. Here, miR-616 mimics could also increase JAK1 and STAT3 phosphorylation levels, and miR-616 inhibitors markedly suppressed the phosphorylation of JAK1 and STAT3 in HEC1A and Ishikawa cells (Fig. 5C). Indeedly, miR-616 mimics inhibited the luciferase activity of the SOCS4 (SOCS5) 3′-UTR reporter plasmids in HEC1A and Ishikawa cells, while the luciferase activities were restored after the predicted miR-616 binding sites were mutated. However, lncRNA-TUSC7 upregulation increased the luciferase activity of the SOCS4 (SOCS5) 3′-UTR reporter plasmids in HEC1A and Ishikawa cells, while the mutation of miR-616 binding sites restored the luciferase activities (Fig. 5E). Western blot results demonstrated that SOCS4 and SOCS5 protein levels were markedly increased after overexpressing lncRNA-TUSC7. Accordingly, TUSC7 upregulation led to significant decreased levels of phosphorylated-JAK1 and STAT3 in HEC1A and Ishikawa cells (Fig. 5F). IHC analysis in clinical specimens showed that SOCS4 (SOCS5) protein levels were markedly decreased in EC tissue samples (Fig. 5G). Pearson's correlation analysis indicated the positive relationships between TUSC7 expression and SOCS4/5 protein levels, and negative relationships between miR-616 and SOCS4 (SOCS5) protein levels in tissue samples of EC patients were found (Fig. 5H). The representative IHC images of SOCS4 (SOCS5) in tissue samples of EC patients were shown in Fig. 5I. Totally, these results suggested that miR-616 might regulate the expression levels of SOCS4 (SOCS5) and phosphorylation of JAK1 and STAT3.

3.4. miR-616/SOCS4 and miR-616/SOCS5 affects proliferation, metastasis and cycle progression of EC cells

Considering the effect of miR-616 on JAK1 and STAT3 phosphorylation, its influence on cell proliferation, metastasis and cycle progression was studied in subsequent experiments. After transfected SOCS4 (SOCS5) expressing plasmids, SOCS4 and SOCS5 mRNA levels were markedly increased, and SOCS4 and SOCS5 protein levels significantly increased in HEC1A and Ishikawa cells (Fig. 6A and B). As Fig. 6C showed, the cell growth was promoted after miR-616 was upregulated, and was inhibited after overexpressing miR-616 and SOCS4 (SOCS5) simultaneously in HEC1A and Ishikawa cells. The colony formation assay results showed that miR-616 overexpression significantly increased colony numbers, and miR-616 + SOCS4 (SOCS5) overexpression inhibited colony formation in HEC1A and Ishikawa cells (Fig. 6D).

The wound scratch healing results showed that the mobility of HEC1A and Ishikawa cells were significantly enhanced after upregulating miR-616, and was markedly reduced after transfection of miR-616 + SOCS4 (SOCS5) (Fig. 6E). As shown in Fig. 6F, invaded HEC1A and Ishikawa cell numbers with miR-616 upregulation were significantly increased, and the numbers of invaded cells with miR-616 + SOCS4 (SOCS5) overexpression were significantly reduced. Additionally, as shown in Fig. 6G, miR-616 overexpression in HEC1A and Ishikawa cells resulted in a distinct decrease in the G1-phase cell population and an increase in the S-phase cell population as compared with the miR-NC + Control cells, which were attenuated after overexpressing miR-616 and SOCS4 (SOCS5) simultaneously. The western blot data in Fig. 6H showed that the altered expression levels of p21, cyclinD1,E-cadherin, MMP2, MMP9 and Vimentin by miR-616 overexpression in HEC1A and Ishikawa cells were significantly attenuated after overexpressing miR-616 and SOCS4 (SOCS5) simultaneously. These results above indicated that miR-616 can promote cell proliferation, cell cycle progression and cell metastasis in HEC1A and Ishikawa cells, which was at least, partially dependent on the inhibition of SOCS4 and SOCS5.

3.5. TUSC7/miR-616 effects the proliferation, metastasis and cycle progression of EC cells

Afterwards, we studied the effects of TUSC7/miR-616 axis in the proliferation, metastasis and cycle progression of HEC1A and Ishikawa cells. The results in Fig. 7A revealed that SOCS4 and SOCS5 protein levels were markedly increased after transfected TUSC7 expressing plasmids, while the simultaneous overexpression of TUSC7 + miR-616 weakened the variability of the protein expressions of SOCS4, SOCS5, p-JAK1 and p-STAT3. As Fig. 7B showed, the cell growth was inhibited after TUSC7 was upregulated, and the effect was abolished after overexpressing TUSC7 and miR-616 simultaneously. The colony formation results showed that TUSC7 overexpression significantly decreased colony numbers, and TUSC7 + miR-616 overexpression eliminated the influence on colony formation (Fig. 7C).

Furthermore, the wound scratch healing results showed that the mobility of HEC1A and Ishikawa cells was significantly inhibited after TUSC7 upregulation, and this effect was markedly reduced after simultaneous transfection of TUSC7 + miR-616 (Fig. 7D). As shown in Fig. 7E, invaded cell numbers with lncRNA-TUSC7 upregulation were significantly decreased, and these results were attenuated by TUSC7 + miR-616 overexpression. Additionally, as shown in Fig. 7F and G, overexpressing TUSC7 + miR-616 simultaneously also notably weakened the effects of TUSC7 overexpression on cell cycle arrest and the expression levels of p21, cyclinD1, E-cadherin, MMP2, MMP9 and Vimentin in HEC1A and Ishikawa cells arrest These results indicated that TUSC7 can suppress cell proliferation, cell cycle progression and cell metastasis in HEC1A and Ishikawa cells, at least partially, through inhibiting miR-616.

3.6. TUSC7 inhibits tumor growth in EC mouse xenograft model

The function of TUSC7/miR-616 axis was finally analyzed *in vivo*, and HEC1A cells stably overexpressing TUSC7 were established for the immunodeficient mouse xenograft tumor model. After two groups of nude mice were subcutaneously implanted with the stable cells, the corresponding tumors were excised and the representative photograph was shown in Fig. 8A. Fig. 8B showed that the weight of the excised

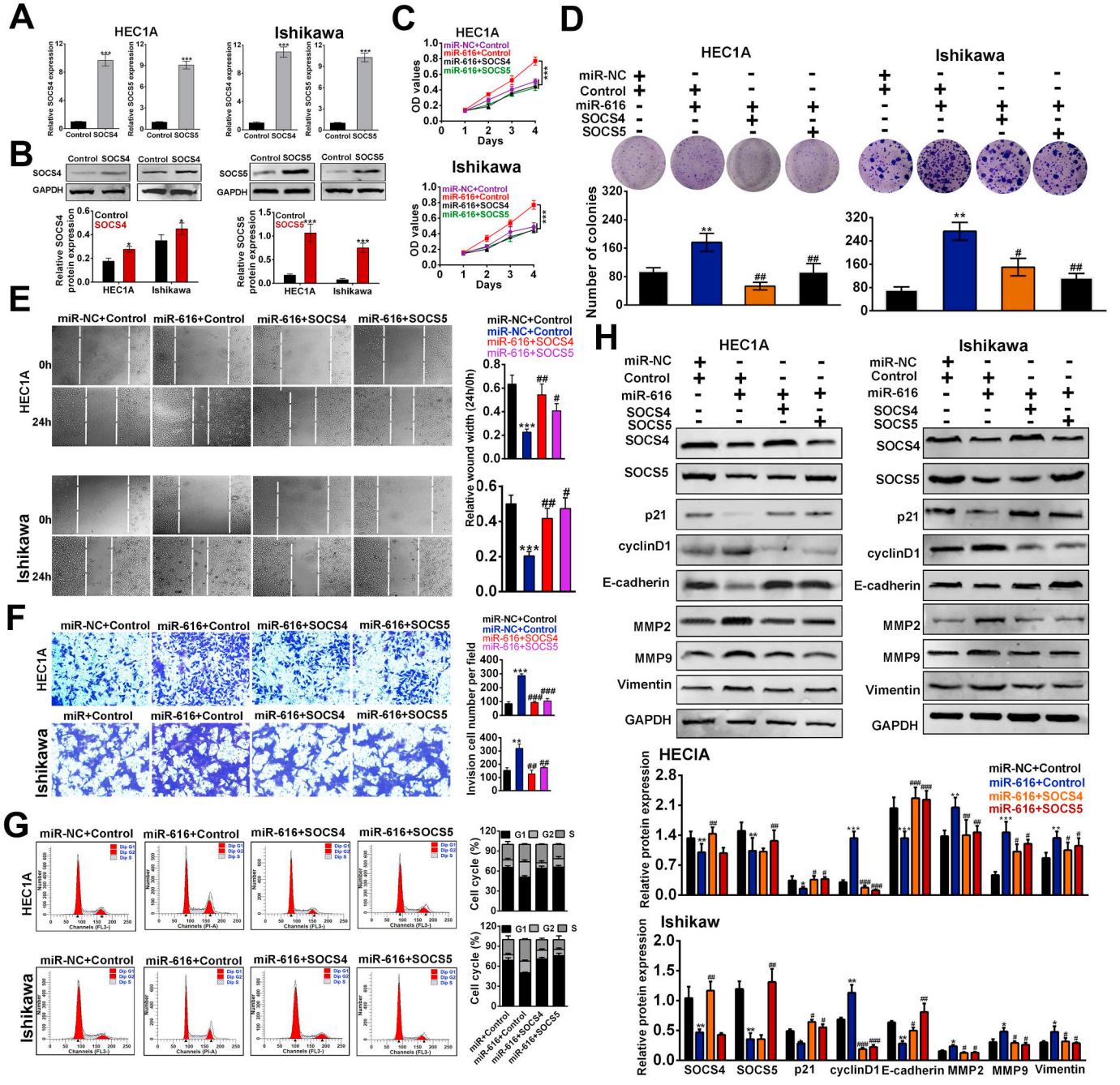

Fig. 6. miR-616/SOCS4 and miR-616/SOCS5 effects the proliferation, metastasis and cycle progression of EC cells. (A) The relative SOCS4 or SOCS5 expression levels in HEC1A or Ishikawa cells after transfection with SOCS4 or SOCS5 expressing plasmids (SOCS4 or SOCS5) or the corresponding control (Control), as determined using qRT-PCR. (B) The protein levels of SOCS4 or SOCS5 in HEC1A or Ishikawa cells after transfection with SOCS4 or SOCS5 expressing plasmids (SOCS4 or SOCS5) or the corresponding control (Control), as determined using western blotting. Relatively quantitative results was determined by Image J and shown as histogram. (C) Growth curves of HEC1A or Ishikawa cells after transfection with miR-616 + Control, miR-616 + SOCS4, miR-616 + SOCS5 or the corresponding control (miR-NC + Control). The measurements of the cell growth rate were obtained using a CCK-8 kit. (D) Colony formation analysis of HEC1A or Ishikawa cells after transfection with miR-616 + Control, miR-616 + SOCS4, miR-616 + SOCS5 or the corresponding control (miR-NC + Control). Colony numbers were quantified and shown as histograms. (E) Wound scratch healing assay of HEC1A or Ishikawa cells after transfection with miR-616 + Control, miR-616 + SOCS4, miR-616 + SOCS5 or the corresponding control (miR-NC + Control). Quantification of the wound-healing assay was shown as histograms. (F) Representative invasion assay images of HEC1A or Ishikawa cells after transfection with miR-616 + Control, miR-616 + SOCS4, miR-616 + SOCS5 or the corresponding control (miR-NC + Control). The invaded cells were quantified and shown as histograms. (G) Cell cycle analysis of HEC1A or Ishikawa cells after transfection with miR-616 + Control, miR-616 + SOCS4, miR-616 + SOCS5 or the corresponding control (miR-NC + Control). Apoptosis rates were quantified and shown as histograms. (H) The protein levels of SOCS4, SOCS5, p21, cyclinD1, E-cadherin, MMP2, MMP9 and Vimentin in HEC1A or Ishikawa cells after transfection with miR-616 + Control, miR-616 + SOCS4, miR-616 + SOCS5 or the corresponding control (miR-NC + Control), as determined using western blotting. Relatively quantitative results was determined by Image J and shown as histogram. The data are expressed as the mean ± SEM, */#P < 0.05; **/##P < 0.01; ***/###P < 0.001.

tumors in lncRNA-TUSC7 group was reduced compared with that of the Con group at 8 weeks post-implantation. And the tumor sizes in the lncRNA-TUSC7 group were significantly smaller than those in the Con groups (Fig. 8C). Histopathological analysis indicated that TUSC7 upregulation decreased the number of Ki-67 positive cells and the Vimentin expression, but caused significant decreased miR-616 expression in xenograft tumors (Fig. 8D). Moreover, western blot results showed that TUSC7 overexpression could upregulate SOCS4 and SOCS5, and downregulate phosphorylation of JAK1 and STAT3 in xenograft tumors (Fig. 8E). These results suggested that the TUSC7 overexpression could downregulate the miR-616 expression, suppress the protein expression of Vimentin, decrease cell proliferation and

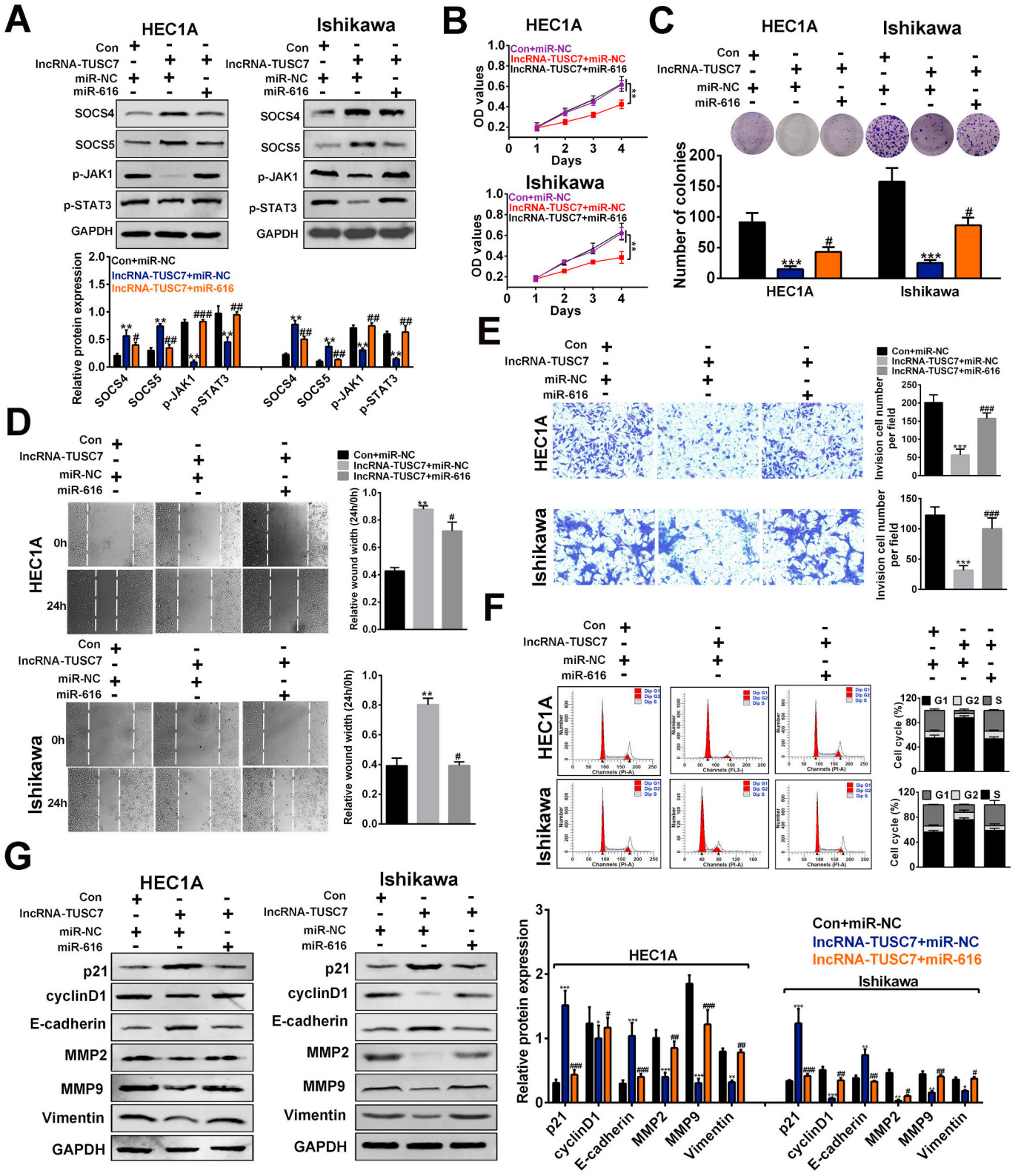

(caption on next page)

Fig. 7. TUSC7/miR-616 effects the proliferation, metastasis and cycle progression of EC cells. (A) The protein levels of SOCS4, SOCS5, p-JAK1 and p-STAT3 in HEC1A or Ishikawa cells after transfection with lncRNA-TUSC7 + miR-NC, lncRNA-TUSC7 + miR-616 or the corresponding control (Con + miR-NC), as determined using western blotting. Relatively quantitative results was determined by Image J and shown as histogram. (B) Growth curves of HEC1A or Ishikawa cells after transfection with lncRNA-TUSC7 + miR-NC, lncRNA-TUSC7 + miR-616 or the corresponding control (Con + miR-NC). The measurements of the cell growth rate were obtained using a CCK-8 kit. (C) Colony formation analysis of HEC1A or Ishikawa cells after transfection with lncRNA-TUSC7 + miR-NC, lncRNA-TUSC7 + miR-616 or the corresponding control (Con + miR-NC). Colony numbers were quantified and shown as histograms. (D) Wound scratch healing assay of HEC1A or Ishikawa cells after transfection with lncRNA-TUSC7 + miR-NC, lncRNA-TUSC7 + miR-616 or the corresponding control (Con + miR-NC). Quantification of the wound-healing assay was shown as histograms. (E) Representative invasion assay images of HEC1A or Ishikawa cells after transfection with lncRNA-TUSC7 + miR-NC, lncRNA-TUSC7 + miR-616 or the corresponding control (Con + miR-NC). The invaded cells were quantified and shown as histograms. (F) Cell cycle analysis of HEC1A or Ishikawa cells after transfection with lncRNA-TUSC7 + miR-NC, lncRNA-TUSC7 + miR-616 or the corresponding control (Con + miR-NC). Apoptosis rates were quantified and shown as histograms. (G) The protein levels of p21, cyclinD1, E-cadherin, MMP2, MMP9 and Vimentin in HEC1A or Ishikawa cells after transfection with lncRNA-TUSC7 + miR-NC, lncRNA-TUSC7 + miR-616 or the corresponding control (Con + miR-NC), as determined using western blotting. Relatively quantitative results was determined by Image J and shown as histogram. The data are expressed as the mean ± SEM, */#P < 0.05; **/##P < 0.01; ***/###P < 0.001.

finally inhibit the EC growth *in vivo* (Fig. 9).

4. Discussion

Here, our results suggested the anti-proliferative, anti-cycle progression and anti-metastatic function of TUSC7, and provided a regulatory relationship between TUSC7 and miR-616/SOCS4 (SOCS5). It was gradually demonstrated that lncRNAs were strongly associated with EC progression. For example, Cui et al. found that increased lncRNA MIR22HG expression significantly inhibited EC cells proliferation, induced EC cells apoptosis, and arrested EC cells in G0/G1 phase, through regulating miR-141-3p/DAPK1 axis [39]. Kong et al. suggested that up-regulated PVT1 and down-regulated miR-195-5p facilitated cell proliferation, migration, and invasion while inhibiting apoptosis of EC cells [40]. Zhang et al. demonstrated that lncRNA H19 overexpression in EC may regulate HOXA10 expression by targeting miR-612, thus promoting cell proliferation in EC development [41]. These findings indicated that lncRNAs usually exert regulatory roles by negatively sponging target miRNAs. In the present study, we demonstrated that miR-616 could be sponged by TUSC7 in EC. In other study, miR-23b was reported to be regulated by TUSC7 in EC and the activation of TUSC7/miR-23b could improve the chemotherapy sensitivity to CDDP and Taxol for EC patients [16]. Except for miR-616 and miR-23b, other miRNAs have been found to be regulated by TUSC7 in several cancers, for instance, miR-211 in colorectal cancer [42] and miR-10a in hepatocellular carcinoma [9]. To our knowledge, the functional role of miR-211 and miR-10a in EC has not been demonstrated. Thus, whether TUSC7 could participate in EC progression by sponging miR-211 and miR-10a needs following investigation. Using the bioinformatics prediction method, Targetscan, the binding sequences between miR-616 and SOCS4 (SOCS5) were found. Previous study demonstrated that as miR-616, a small noncoding RNA, can function as an oncogene in some cancer cells by targeting miRNAs. It was indicated that miR-616 could promote cell proliferation both in non-small cell lung cancer and glioma

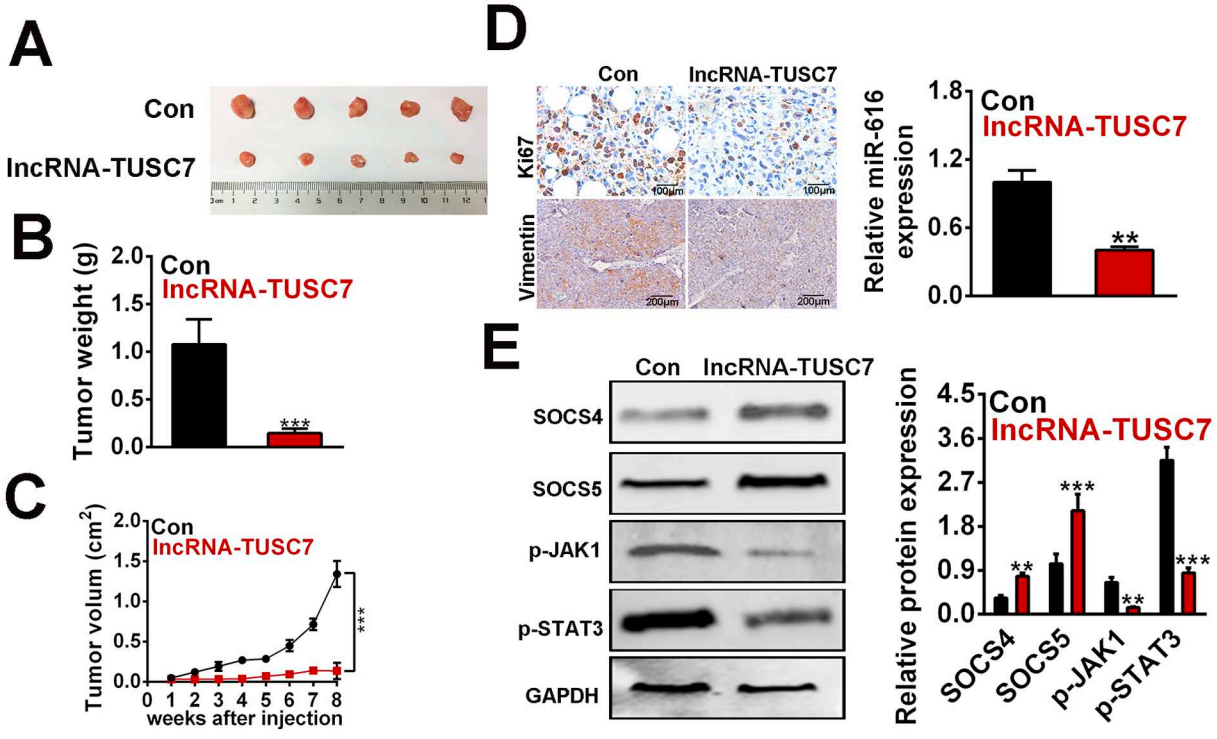

Fig. 8. TUSC7 inhibits tumor growth in an EC mouse xenograft model. (A) A representative photograph of corresponding tumors dissected from mice at 8 weeks post-implantation. (B) The weights of the xenograft tumors in nude mice derived from subcutaneous implantation of HEC1A cells stably expressing TUSC7 or the control cells (Con). (C) The volumes of the xenograft tumors of nude mice derived from subcutaneous implantation of HEC1A cells stably expressing TUSC7 or the control cells (Con). (D) Immunohistochemical staining of Ki67 and Vimentin, and qRT-PCR of miR-616 in the xenograft tumors in nude mice derived from subcutaneous implantation of HEC1A cells stably expressing TUSC7 or the control cells (Con). (E) The protein levels of SOCS4, SOCS5, p-JAK1 and p-STAT3 in the xenograft tumors in nude mice derived from subcutaneous implantation of HEC1A cells stably expressing TUSC7 or the control cells (Con), as determined using western blotting. Relatively quantitative results was determined by Image J and shown as histogram. The data are expressed as the mean ± SEM, **P < 0.01; ***P < 0.001.

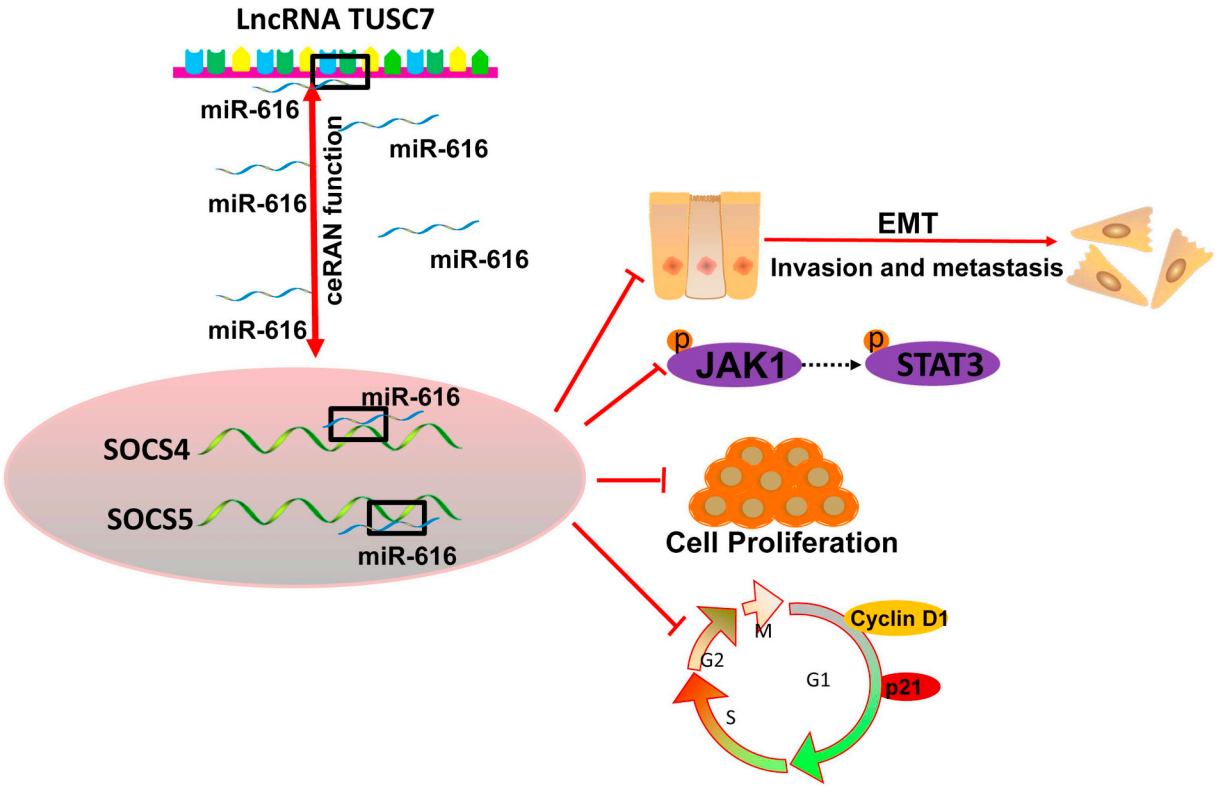

Fig. 9. Model of lncRNA TUSC7 signal transduction. Following sponging miR-616, lncRNA TUSC7 upregulates the protein expressions of SOCS4 and SOCS5, suppresses the phosphorylation of JAK1 and STAT3, and further inhibits cell proliferation, metastasis, EMT and cell cycle progression in EC development.

cells through targeting SOX7 [21,22]. Other cancer-related genes, mainly including TFPI-2 in prostate cancer [21], PTEN in hepatocellular carcinoma [22] and GSK3β in lung cancer [17], have been also revealed to be regulated by miR-616,. Among the determined targets of miR-616 (SOX7, TFPI-2, PTEN and GSK3β), GSK-3β was overexpressed in EC tissues, and overexpressed GSK-3β could predict lower cumulative and relapse-free survival rate of EC patients [43], which arises the possibility that miR-616 might be involved in EC progression by regulating GSK-3β expression. SOX7 is identified as a negative regulator of Wnt/β-catenin signaling pathway through impeding the transcriptional machinery of β-catenin/TCF/LEF-1 transcriptional complex in EC [44]. PTEN' expression was demonstrated to be significantly decreased in EC, and negatively correlated to the expression of miR-181a [45]. Thus, it seems that SOX7 and PTEN may function as tumor suppressors in EC. Our data showed that miR-616 could probably interact with 3′-UTR of SOCS4 (SOCS5) and negatively regulate their protein expressions. Taken together, it might be hypothesized that miR-616 exerts its regulatory activity in EC by regulating various target genes, SOCS4, SOCS5, SOX7 or PTEN, which might be explore in further analysis.

Moreover, overexpressing TUSC7 + miR-616 simultaneously notably weakened the effects of TUSC7 overexpression on cell proliferation, cell cycle progression and cell metastasis in HEC1A and Ishikawa cells, indicating that TUSC7 can suppress cell proliferation, cell cycle progression and cell metastasis in HEC1A and Ishikawa cells, at least partially, through inhibiting miR-616. The present also showed that overexpressing miR-616 and SOCS4 (SOCS5) simultaneously significantly attenuated the effects of miR-616 overexpression on cell proliferation, cell cycle progression and cell metastasis in HEC1A and Ishikawa cells. These investigations suggested that miR-616 can promote cell proliferation, cell cycle progression and cell metastasis in HEC1A and Ishikawa cells, which was at least, partially dependent on the inhibition of SOCS4 and SOCS5.Thus, we concluded that the process of TUSC7/miR-616 in influencing cell proliferation, cycle progression and metastasis was involved in the regulation of SOCS4 (SOCS5).

As important negative feedback regulators of cytokine signaling, SOCS proteins have been recently demonstrated to play important roles in different cancers. Previous studies have provided few evidences about SOCS4 and SOCS5, which focus merely on the dysregulation of SOCS4 in gastric cancer and SOCS5 in thyroid gland cancer and liver cancer [31,32]. This is the first evidence demonstrating the roles of SOCS4 and SOCS5 in EC. SOCS are well-known to control the magnitude and duration of JAK/STAT signaling through several mechanisms, including JAK inhibition, STAT binding and targeting for proteasomal degradation [24,37,38]. Consistently, our results showed that the phosphorylation levels of JAK and STAT3 were significantly upregulated, after SOCS4 and SOCS5 were inhibited by miR-616 overexpression. It suggested that miR-616 can influence cell proliferation, cycle and metastasis though suppressing the expression of SOCS4 and SOCS5 in EC cells by targeting their 3′-UTR, and thus, the phosphorylation levels of JAK and STAT3 were significantly upregulated.

Except for miR-616, no miRNA and lncRNA have been reported to simultaneously regulate SOCS4 and SOCS5 at post-transcriptional level in EC. Nevertheless, some miRNAs have been reported to target SOCS4 or SOCS5 in other diseases. For SOCS4, miR-1290 in lung cancer [46], miR-25 in thyroid cancer [33] and miR-98 and let-7 in biliary epithelial cells in response to *Cryptosporidium parvum* infection [47] are identified as its important post-transcriptional regulators. Additionally, SOCS5 can be targeted and negatively by miR-124 in $CD4^+$ T cells [48], miR-302a-3p in pancreatic cancer [49], miRNA-432 in Japanese encephalitis virus pathogenesis [50] and miR-132 in chronic obstructive pulmonary disease [51], *etc.* Based on the characteristic that one gene could be regulated by multi-miRNAs, further studies are needed to illustrate whether other miRNAs could simultaneously target SOCS4 and SOCS5 in EC, which may help to understand the mechanism underlying the dysregulation of SOCS4 and SOCS5 in EC.

In summary, our findings revealed that lncRNA TUSC7 downexpression can suppress cell proliferation, cell cycle progression and cell metastasis in HEC1A and Ishikawa cells. TUSC7 could

competitively sponge miR-616 and decrease its expression. Additionally, TUSC7/miR-616 played an important role in regulating the expression of SOCS4 and SOCS5 in EC by targeting its 3′-UTR. Furthermore, TUSC7 overexpression can downregulate the miR-616 expression and inhibit tumor growth in an EC mouse xenograft model. Based on the function of anti-proliferation, anti-cell cycle progression and anti-metastasis, the signaling axis of lncRNA TUSC7/miR-616/SOCS4 (SOCS5) may hold promise as a promising target in EC treatment.

Declaration of Competing Interests

The authors declare that they have no competing interests, and all authors should confirm its accuracy.

Acknowledgements

Not applicable.

Funding

This work was supported by the National Natural Science Foundation of China (Grant No. 81702578).

References

[1] R.L. Siegel, K.D. Miller, A. Jemal, Cancer statistics, 2018, CA Cancer J. Clin. 68 (1) (2018) 7–30, https://doi.org/10.3322/caac.21442 (29313949).
[2] J.D. Wright, N.I. Barrena Medel, J. Sehouli, K. Fujiwara, T.J. Herzog, Contemporary management of endometrial cancer, Lancet 379 (9823) (2012) 1352–1360, https://doi.org/10.1016/S0140-6736(12)60442-5 (PMID: 22444602).
[3] K. Matsuo, A.A. Ramzan, M.R. Gualtieri, P. Mhawech-Fauceglia, H. Machida, A. Moeini, C.E. Dancz, Y. Ueda, L.D. Roman, Prediction of concurrent endometrial carcinoma in women with endometrial hyperplasia, Gynecol. Oncol. 139 (2) (2015) 261–267, https://doi.org/10.1016/j.ygyno.2015.07.108 (26238457).
[4] J. Al-Maghrabi, A. Abdelrahman, B. Al-Maghrabi, A. Buhmeida, A. Abuzenadah, M. Al-Qahtani, M. Al-Ahwal, M.J.E.J.O.G.O. Khabaz, Loss of p27 Expression in Endometrial Carcinoma Patients With Recurrent Tumor is Significantly Associated With Poor Survival, 39(1) (2018), pp. 119–123 (DOI: PMID:).
[5] A. Rafiee, F. Riazi-Rad, M. Havaskary, F. Nuri, Long noncoding RNAs: regulation, function and cancer, Biotechnol Genet Eng Rev 34 (2) (2018) 153–180, https://doi.org/10.1080/02648725.2018.1471566 (30071765).
[6] N. Coccaro, A. Zagaria, G. Tota, L. Anelli, P. Orsini, P. Casieri, A. Cellamare, A. Minervini, L. Impera, C.F. Minervini, et al., Overexpression of the LSAMP and TUSC7 genes in acute myeloid leukemia following microdeletion/duplication of chromosome 3, Cancer Genet 208 (10) (2015) 517–522, https://doi.org/10.1016/j.cancergen.2015.07.006 (26345353).
[7] N. Li, M. Yang, K. Shi, W. Li, Prognostic value of decreased long non-coding RNA TUSC7 expression in some solid tumors: a systematic review and meta-analysis, Oncotarget 8 (35) (2017) 59518–59526, https://doi.org/10.18632/oncotarget.18496 (PMID: 28938655.).
[8] X.S. Shi, Y.S. Chen, A.M. Chen, X.B. Le, K.L. Huang, J.Y. Chen, S. Wen, H.K. Zeng, C. Chen, J. Li, LncRNA TUSC7 affects malignant tumor prognosis by regulating protein ubiquitination: a genome-wide analysis from 10,237 pan-cancer patients, Transl. Cancer Res. 6 (4) (2017), https://doi.org/10.21037/tcr.2017.08.19 834-+.. (PMID: WOS:000409349600018).
[9] Y. Wang, Z. Liu, B. Yao, C. Dou, M. Xu, Y. Xue, L. Ding, Y. Jia, H. Zhang, Q. Li, et al., Long non-coding RNA TUSC7 acts a molecular sponge for miR-10a and suppresses EMT in hepatocellular carcinoma, Tumour Biol. 37 (8) (2016) 11429–11441, https://doi.org/10.1007/s13277-016-4892-6 (27002617).
[10] X.L. Ma, W.D. Zhu, L.X. Tian, W.D. Sun, F. Shang, Q.T. Lin, H.Q. Zhang, Long non-coding RNA TUSC7 expression is independently predictive of outcome in glioma, Eur. Rev. Med. Pharmacol. Sci. 21 (16) (2017) 3605–3610 (DOI: PMID: 28925483).
[11] P. Qi, M.D. Xu, X.H. Shen, S.J. Ni, D. Huang, C. Tan, W.W. Weng, W.Q. Sheng, X.Y. Zhou, X. Du, Reciprocal repression between TUSC7 and miR-23b in gastric cancer, Int. J. Cancer 137 (6) (2015) 1269–1278, https://doi.org/10.1002/ijc.29516 (25765901).
[12] C. Shang, Y. Guo, Y. Hong, Y.X. Xue, Long non-coding RNA TUSC7, a target of miR-23b, plays tumor-suppressing roles in human gliomas, Front. Cell. Neurosci. 10 (2016) 235, https://doi.org/10.3389/fncel.2016.00235 (PMID: 27766072.).
[13] M. Cong, J. Li, R. Jing, Z. Li, Long non-coding RNA tumor suppressor candidate 7 functions as a tumor suppressor and inhibits proliferation in osteosarcoma, Tumour Biol. 37 (7) (2016) 9441–9450, https://doi.org/10.1007/s13277-015-4414-y (26781978).
[14] W. Ren, S. Chen, G. Liu, X. Wang, H. Ye, Y. Xi, TUSC7 acts as a tumor suppressor in colorectal cancer, Am. J. Transl. Res. 9 (9) (2017) 4026–4035 (DOI: PMID: 28979678).
[15] Z. Wang, Y. Jin, H. Ren, X. Ma, B. Wang, Y. Wang, Downregulation of the long non-coding RNA TUSC7 promotes NSCLC cell proliferation and correlates with poor prognosis, Am. J. Transl. Res. 8 (2) (2016) 680–687 (. DOI: PMID: 27158360).
[16] C. Shang, B. Lang, C.N. Ao, L. Meng, Long non-coding RNA tumor suppressor candidate 7 advances chemotherapy sensitivity of endometrial carcinoma through targeted silencing of miR-23b, Tumour Biol. 39 (6) (2017), https://doi.org/10.1177/1010428317707883 (PMID: 28653877.).
[17] S. Ma, Y.P. Chan, P.S. Kwan, T.K. Lee, M. Yan, K.H. Tang, M.T. Ling, J.R. Vielkind, X.Y. Guan, K.W. Chan, MicroRNA-616 induces androgen-independent growth of prostate cancer cells by suppressing expression of tissue factor pathway inhibitor TFPI-2, Cancer Res. 71 (2) (2011) 583–592, https://doi.org/10.1158/0008-5472.CAN-10-2587 (PMID: 21224345).
[18] Y. Yao, A.L. Suo, Z.F. Li, L.Y. Liu, T. Tian, L. Ni, W.G. Zhang, K.J. Nan, T.S. Song, C. Huang, MicroRNA profiling of human gastric cancer, Mol. Med. Rep. 2 (6) (2009) 963–970 (DOI:10.3892/mmr_00000199 PMID: 21475928.).
[19] M. Garofalo, G. Romano, G. Di Leva, G. Nuovo, Y.J. Jeon, A. Ngankeu, J. Sun, F. Lovat, H. Alder, G. Condorelli, et al., EGFR and MET receptor tyrosine kinase-altered microRNA expression induces tumorigenesis and gefitinib resistance in lung cancers, Nat. Med. 18 (1) (2011) 74–82, https://doi.org/10.1038/nm.2577 (22157681).
[20] D. Zhang, P. Zhou, W. Wang, X. Wang, J. Li, X. Sun, L. Zhang, MicroRNA-616 promotes the migration, invasion and epithelial-mesenchymal transition of HCC by targeting PTEN, Oncol. Rep. 35 (1) (2016) 366–374, https://doi.org/10.3892/or.2015.4334 (26499912).
[21] D. Wang, Q. Cao, M. Qu, Z. Xiao, M. Zhang, S. Di, MicroRNA-616 promotes the growth and metastasis of non-small cell lung cancer by targeting SOX7, Oncol. Rep. 38 (4) (2017) 2078–2086, https://doi.org/10.3892/or.2017.5854 (28765960).
[22] Q.L. Bai, C.W. Hu, X.R. Wang, J.X. Shang, G.F. Yin, MiR-616 promotes proliferation and inhibits apoptosis in glioma cells by suppressing expression of SOX7 via the Wnt signaling pathway, Eur. Rev. Med. Pharmacol. Sci. 21 (24) (2017) 5630–5637, https://doi.org/10.26355/eurrev_201712_14006 (PMID: 29271996).
[23] W.S. Alexander, Suppressors of cytokine signalling (SOCS) in the immune system, Nat Rev Immunol 2 (6) (2002) 410–416, https://doi.org/10.1038/nri818 (12093007).
[24] M.C. Trengove, A.C. Ward, SOCS proteins in development and disease, Am J Clin Exp Immunol 2 (1) (2013) 1–29 (DOI: PMID: 23885323).
[25] P.A. Ram, D.J. Waxman, SOCS/CIS protein inhibition of growth hormone-stimulated STAT5 signaling by multiple mechanisms, J. Biol. Chem. 274 (50) (1999) 35553–35561 (10585430).
[26] B.T. Kile, B.A. Schulman, W.S. Alexander, N.A. Nicola, H.M. Martin, D.J. Hilton, The SOCS box: a tale of destruction and degradation, Trends Biochem. Sci. 27 (5) (2002) 235–241 (12076535).
[27] B. He, L. You, K. Uematsu, K. Zang, Z. Xu, A.Y. Lee, J.F. Costello, F. McCormick, D.M. Jablons, SOCS-3 is frequently silenced by hypermethylation and suppresses cell growth in human lung cancer, Proc. Natl. Acad. Sci. U. S. A. 100 (24) (2003) 14133–14138, https://doi.org/10.1073/pnas.2232790100 (14617776).
[28] K.F. To, M.W. Chan, W.K. Leung, E.K. Ng, J. Yu, A.H. Bai, A.W. Lo, S.H. Chu, J.H. Tong, K.W. Lo, et al., Constitutional activation of IL-6-mediated JAK/STAT pathway through hypermethylation of SOCS-1 in human gastric cancer cell line, Br. J. Cancer 91 (7) (2004) 1335–1341, https://doi.org/10.1038/sj.bjc.6602133 (15354212).
[29] A. Weber, U.R. Hengge, W. Bardenheuer, I. Tischoff, F. Sommerer, A. Markwarth, A. Dietz, C. Wittekind, A. Tannapfel, SOCS-3 is frequently methylated in head and neck squamous cell carcinoma and its precursor lesions and causes growth inhibition, Oncogene 24 (44) (2005) 6699–6708, https://doi.org/10.1038/sj.onc.1208818 (16007169).
[30] I. Storojeva, J.L. Boulay, P. Ballabeni, M. Buess, L. Terracciano, U. Laffer, G. Mild, R. Herrmann, C. Rochlitz, Prognostic and predictive relevance of DNAM-1, SOCS6 and CADH-7 genes on chromosome 18q in colorectal cancer, Oncology 68 (2–3) (2005) 246–255, https://doi.org/10.1159/000086781 (16015041).
[31] D. Kobayashi, S. Nomoto, Y. Kodera, M. Fujiwara, M. Koike, G. Nakayama, N. Ohashi, A. Nakao, Suppressor of cytokine signaling 4 detected as a novel gastric cancer suppressor gene using double combination array analysis, World J. Surg. 36 (2) (2012) 362–372, https://doi.org/10.1007/s00268-011-1358-2 (22127425).
[32] S. Yoon, Y.S. Yi, S.S. Kim, J.H. Kim, W.S. Park, S.W. Nam, SOCS5 and SOCS6 have similar expression patterns in normal and cancer tissues, Tumour Biol. 33 (1) (2012) 215–221, https://doi.org/10.1007/s13277-011-0264-4 (22081311).
[33] Z. Mei, S. Chen, C. Chen, B. Xiao, F. Li, Y. Wang, Z. Tao, Interleukin-23 facilitates thyroid cancer cell migration and invasion by inhibiting SOCS4 expression via microRNA-25, PLoS One 10 (10) (2015) e0139456, , https://doi.org/10.1371/journal.pone.0139456 (26437444).
[34] A. World Medical, World Medical Association Declaration of Helsinki: ethical principles for medical research involving human subjects, JAMA 310 (20) (2013) 2191–2194, https://doi.org/10.1001/jama.2013.281053 (PMID: 24141714).
[35] G. Ma, M. Tang, Y. Wu, X. Xu, F. Pan, R. Xu, LncRNAs and miRNAs: potential biomarkers and therapeutic targets for prostate cancer, Am. J. Transl. Res. 8 (12) (2016) 5141–5150 (. DOI: PMID: 28077991).
[36] E. Alleva, D. Santucci, Guide for the care and use of laboratory animals, Ethology 103 (12) (1997) 1072–1073 (. DOI: PMID: WOS:000071145900012).
[37] T. Tamiya, I. Kashiwagi, R. Takahashi, H. Yasukawa, A. Yoshimura, Suppressors of cytokine signaling (SOCS) proteins and JAK/STAT pathways: regulation of T-cell inflammation by SOCS1 and SOCS3, Arterioscler. Thromb. Vasc. Biol. 31 (5) (2011) 980–985, https://doi.org/10.1161/ATVBAHA.110.207464 (21508344).
[38] H. Kiu, S.E. Nicholson, Biology and significance of the JAK/STAT signalling pathways, Growth Factors 30 (2) (2012) 88–106, https://doi.org/10.3109/08977194.2012.660936 (22339650).
[39] Z. Cui, X. An, J. Li, Q. Liu, W. Liu, LncRNA MIR22HG negatively regulates miR-141-3p to enhance DAPK1 expression and inhibits endometrial carcinoma cells proliferation, Biomed. Pharmacother. 104 (2018) 223–228, https://doi.org/10.1016/j.

biopha.2018.05.046 (29775889).
[40] F. Kong, J. Ma, H. Yang, D. Yang, C. Wang, X. Ma, Long non-coding RNA PVT1 promotes malignancy in human endometrial carcinoma cells through negative regulation of miR-195-5p, Biochim Biophys Acta Mol Cell Res (2018), https://doi.org/10.1016/j.bbamcr.2018.07.008 (30031900).
[41] L. Zhang, D.L. Wang, P. Yu, LncRNA H19 regulates the expression of its target gene HOXA10 in endometrial carcinoma through competing with miR-612, Eur. Rev. Med. Pharmacol. Sci. 22 (15) (2018) 4820–4827, https://doi.org/10.26355/eurrev_201808_15617 (PMID: 30070313).
[42] J. Xu, R. Zhang, J. Zhao, The novel long noncoding RNA TUSC7 inhibits proliferation by sponging MiR-211 in colorectal cancer, Cell. Physiol. Biochem. 41 (2) (2017) 635–644, https://doi.org/10.1159/000457938 (28214867).
[43] S. Chen, K.X. Sun, B.L. Liu, Z.H. Zong, Y. Zhao, The role of glycogen synthase kinase-3beta (GSK-3beta) in endometrial carcinoma: a carcinogenesis, progression, prognosis, and target therapy marker, Oncotarget 7 (19) (2016) 27538–27551, https://doi.org/10.18632/oncotarget.8485 (PMID: 27050373).
[44] D.W. Chan, C.S. Mak, T.H. Leung, K.K. Chan, H.Y. Ngan, Down-regulation of Sox7 is associated with aberrant activation of Wnt/b-catenin signaling in endometrial cancer, Oncotarget 3 (12) (2012) 1546–1556, https://doi.org/10.18632/oncotarget.667 (PMID: 23295859).
[45] N.S. Geletina, V.S. Kobelev, E.V. Babayants, L. Feng, V.O. Pustylnyak, L.F. Gulyaeva, PTEN negative correlates with miR-181a in tumour tissues of non-obese endometrial cancer patients, Gene 655 (2018) 20–24, https://doi.org/10.1016/j.gene.2018.02.051 (29477866).
[46] X. Xiao, D. Yang, X. Gong, D. Mo, S. Pan, J. Xu, miR-1290 promotes lung adenocarcinoma cell proliferation and invasion by targeting SOCS4, Oncotarget 9 (15) (2018) 11977–11988, https://doi.org/10.18632/oncotarget.24046 (PMID: 29552286).
[47] G. Hu, R. Zhou, J. Liu, A.Y. Gong, X.M. Chen, MicroRNA-98 and let-7 regulate expression of suppressor of cytokine signaling 4 in biliary epithelial cells in response to Cryptosporidium parvum infection, J. Infect. Dis. 202 (1) (2010) 125–135, https://doi.org/10.1086/653212 (PMID: 20486857).
[48] S. Jiang, C. Li, G. McRae, E. Lykken, J. Sevilla, S.Q. Liu, Y. Wan, Q.J. Li, MeCP2 reinforces STAT3 signaling and the generation of effector CD4+ T cells by promoting miR-124-mediated suppression of SOCS5, Sci. Signal. 7 (316) (2014) ra25, https://doi.org/10.1126/scisignal.2004824 (24619648).
[49] Z. Zhang, J. Li, H. Guo, F. Wang, L. Ma, C. Du, Y. Wang, Q. Wang, M. Kornmann, X. Tian, et al., BRM transcriptionally regulates miR-302a-3p to target SOCS5/STAT3 signaling axis to potentiate pancreatic cancer metastasis, Cancer Lett. (2019) 30790683, , https://doi.org/10.1016/j.canlet.2019.02.031.
[50] N. Sharma, K.L. Kumawat, M. Rastogi, A. Basu, S.K. Singh, Japanese encephalitis virus exploits the microRNA-432 to regulate the expression of suppressor of cytokine signaling (SOCS) 5, Sci. Rep. 6 (2016) 27685, , https://doi.org/10.1038/srep27685 (27282499).
[51] X. Diao, J. Zhou, S. Wang, X. Ma, Upregulation of miR-132 contributes to the pathophysiology of COPD via targeting SOCS5, Exp. Mol. Pathol. 105 (3) (2018) 285–292, https://doi.org/10.1016/j.yexmp.2018.10.002 (30292646).